THE JOURNAL OF BIOLOGICAL CHEMISTRY VOL. 287, NO. 43, pp. 36239–36250, October 19, 2012
© 2012 by The American Society for Biochemistry and Molecular Biology, Inc. Published in the U.S.A.

Unconventional Chemiosmotic Coupling of NHA2, a Mammalian Na^+/H^+ Antiporter, to a Plasma Membrane H^+ Gradient*

Received for publication, July 21, 2012, and in revised form, August 25, 2012 Published, JBC Papers in Press, September 4, 2012, DOI 10.1074/jbc.M112.403550

Kalyan C. Kondapalli, Laura M. Kallay, Melanie Muszelik, and Rajini Rao[1]

From the Department of Physiology, The Johns Hopkins University School of Medicine, Baltimore, Maryland 21205

Background: Inwardly directed Na^+ gradients have failed to reveal transport activity of NHA2 in mammalian cells, although it functionally complements salt tolerance in yeast.
Results: NHA2 mediates sodium-lithium countertransport, and cation efflux using an inwardly directed H^+ gradient.
Conclusion: NHA2 is chemiosmotically coupled to the V-ATPase.
Significance: H^+-driven salt and pH homeostasis in the kidney may be important in hypertension.

Human NHA2, a newly discovered cation proton antiporter, is implicated in essential hypertension by gene linkage analysis. We show that NHA2 mediates phloretin-sensitive Na^+-Li^+ counter-transport (SLC) activity, an established marker for hypertension. In contrast to bacteria and fungi where H^+ gradients drive uptake of metabolites, secondary transport at the plasma membrane of mammalian cells is coupled to the Na^+ electrochemical gradient. Our findings challenge this paradigm by showing coupling of NHA2 and V-type H^+-ATPase at the plasma membrane of kidney-derived MDCK cells, resulting in a virtual Na^+ efflux pump. Thus, NHA2 functionally recapitulates an ancient shared evolutionary origin with bacterial NhaA. Although plasma membrane H^+ gradients have been observed in some specialized mammalian cells, the ubiquitous tissue distribution of NHA2 suggests that H^+-coupled transport is more widespread. The coexistence of Na^+ and H^+-driven chemiosmotic circuits has implications for salt and pH regulation in the kidney.

Recently, we identified a novel human gene, *NHA2* (*NHEDC2*, *SLC9B2*), belonging to the cation/proton antiporter (CPA)[2] superfamily, located within a chromosomal region (4q24) associated with hypertension and Na^+-Li^+ countertransport (SLC) activity in numerous linkage studies (1). Hypertension is a major disorder affecting 1 in 4 adults in the United States, with increased renal sodium reabsorption as an established risk factor (2). SLC activity is an established clinical marker for essential hypertension and a highly heritable trait. Since elevated SLC activity in erythrocytes from hypertensive patients correlated with increased renal reabsorption of sodium (3), it presents a potential therapeutic target in the management of hypertension. It is likely that SLC represents an alternate mode of Na^+-H^+ exchange (3), however, the molecular identity of the transporter is still unknown. Of note, a role for the ubiquitous and well-characterized Na^+/H^+ exchanger NHE1 has been ruled out by linkage and inhibitor studies (4).

Heterologous expression of NHA2 in yeast complemented salt-sensitive growth phenotypes and revealed characteristic features of SLC including cation selectivity for Na^+ and Li^+ (but not K^+), insensitivity to amiloride (a hallmark of plasma membrane NHE) and sensitivity to phloretin and quinidine (1, 5, 6). In mammals, NHA2 is expressed in erythrocytes and a wide range of tissues, with high levels detected in the distal tubules of the kidney nephron (7). Although the distal segments of the nephron reabsorb less than 10% of the filtered load of sodium, this region responds to dietary sodium intake and is subject to hormonal control, with subsequent up- or down-regulation of Na^+ transporters and channels to fine tune renal Na^+ reabsorption (8). Taken together, the evidence points to a potential critical role for NHA2 in salt homeostasis.

Despite the promising complementation studies in yeast, functional evidence of NHA2 transport activity in mammalian cells was lacking. Moe and co-workers (7) introduced NHA2 into mammalian cell lines devoid of endogenous NHE1 and reportedly failed to detect Na^+-driven H^+ efflux, the conventional mode expected for mammalian secondary transport. Therefore, we reasoned that there must be fundamental mechanistic differences between NHA2 and NHE antiport. Phylogenetic analysis places metazoan NHA2 in a clade distinct from the NHE cluster, and more closely related in sequence to bacterial NhaA (1). In contrast to mammalian NHE1 that is powered by the inwardly directed Na^+ gradient to extrude H^+ from the cell, bacterial NhaA is driven by a primary H^+ gradient to function in the direction of Na^+ efflux (9). We noted that this is similar to prevailing chemiosmotic circuits in yeast, where we observed H^+-driven cation extrusion by NHA2. Furthermore, whereas NHE mediates electroneutral Na^+/H^+ exchange, NhaA is electrogenic, with a $2H^+/Na^+$ stoichiometry (10). Finally, although both NHE and NhaA antiporters are highly pH-sensitive, their regulation is in opposite directions: thus, NHE is activated by acid pH, NhaA from *Escherichia coli* is

* This work was supported, in whole or in part, by National Institutes of Health Grants DK054214 (to R. R.) and American Heart Association Grant 11POST7380034 (to K. C. K.).
[1] To whom correspondence should be addressed: Department of Physiology, The Johns Hopkins University School of Medicine, 725 N. Wolfe Street, Baltimore, MD. Tel.: 410-955-4732; E-mail: rrao@jhmi.edu.
[2] The abbreviations used are: CPA, cation/proton antiporter; SLC, Na^+-Li^+ countertransport; AM, acetoxymethyl; MDCK, Madin-Darby canine kidney.

"acid-locked" or inactive below pH 6.5, and demonstrates an increase in rate by three orders of magnitude between pH 7 and 8.5 (11). These differences could contribute to the failure to detect NHA2 activity in mammalian cells.

Here, we provide evidence supporting unusual functional coupling of NHA2 to a proton motive force generated by the V-type H^+-ATPase at the plasma membrane of mammalian cells. Thus, in contrast to the vast majority of sodium-coupled transporters, mammalian NHA2 recapitulates its phylogenetic origins with bacterial orthologs. This unique chemiosmotic coupling results in a virtual cation-H^+ efflux pump with physiological implications for Na^+ and pH homeostasis in the kidney.

EXPERIMENTAL PROCEDURES

Chemicals, Reagents, and Antibodies

Amiloride hydrochloride hydrate (catalogue no. A7410), phloretin (catalogue no. P7912), Ouabain (catalogue no. O-3125), Bumetanide (B 3023), DIDS (D3514), were all purchased from Sigma. MTS assay reagent (G358A) was purchased from Promega. Polyclonal antibodies were raised in rabbit against a 15-aa peptide of HsNHA2 as described previously (1). V-ATPase antibodies were purchased from Santa Cruz Biotechnology, Inc.

Generating Stable MDCK Line Overexpressing GFP-HsNHA2

On day 1, MDCK cells were plated in a 6-well plate at ~30% confluence. After 24 h, the cells were transfected with pEGFPC2 vector carrying human NHA2 tagged to GFP at the N terminus. The following day, the transfected cells were split into 10-cm plates at different dilutions. G418 (final concentration of 200 μg/ml) was added to the plates after 24 h to select for transfected cells. The concentration of the antibiotic was increased to 400 μg/ml the next day. Antibiotic containing media was changed every 2 days for a week; well-isolated clones were selected and then transferred to a 24-well plate. Following selection (400 μg/ml G418) for 72 h, isolated clones were moved to a 6-well plate and high expressing clone was selected by testing the GFP expression on a Western blot and also by microscopy.

Immunofluorescence

Cells were grown in 6-well plates containing glass coverslips (22 × 22 mm) and probed with modifications from a previously published staining protocol (12). A monolayer of MDCK cells were pre-extracted with a solution of PHEM buffer (60 mM PIPES, 25 mM HEPES, 10 mM EGTA, and 2 mM $MgCl_2$, pH 6.8) containing 0.025% saponin for 2 min. The coverslips were washed twice for 2 min with a solution of PHEM buffer containing 0.025% saponin and 8% sucrose. The cells were fixed with a solution of 4% PFA and 8% sucrose in PBS for 30 min at room temperature. Coverslips were rinsed three times quickly to rehydrate, and then three times for 5 min each with PBS. A solution of 1% BSA and 0.025% saponin in PBS was used to block for 1 h. The coverslips were probed with the following primary antibodies in the blocking solution for 1 h: A) E-cadherin (Transduction Laboratories/BD Biosciences) at 1:50 dilution or B) ZO-1 1:500 (Transduction Laboratories/BD Biosciences) or C) V-ATPase a1 (Santa Cruz Biotechnology, INC.) at a dilution of 1:100 After incubation with primary antibodies, coverslips were washed three times for 5 min with 0.2% BSA in PBS. Anti-mouse and anti-rabbit Alexa Fluor 568 at dilutions of 1:1000 (Invitrogen, Carlsbad, CA) were used as secondary antibodies. For immunostaining with NHA2 antibody (1:100 dilution) raised in rabbit against a 15-aa peptide of HsNHA2 (1), a similar protocol was used. The coverslips were incubated in DAPI/PBS (5 mg/ml) for 10 s and rinsed with H_2O and subsequently mounted with Dako Cytomation Fluorescent Mounting Medium (Invitrogen). Cells were imaged on a Zeiss 710NLO Meta confocal microscope.

RT-PCR

mRNA was isolated from control and MDCK stable cells using RNeasy Mini kit from Qiagen following manufacturer's instructions. RNA was treated with DNase I (1 unit for 1 μg RNA; Roche) following which the DNA was inactivated by 25 mM EDTA (final concentration of 3 mM) at 65 °C for 10 min. RNA was reverse transcribed using 0.6 μg/μl random primers (Invitrogen) and superscript III reverse transcriptase (200 units/μl; Invitrogen) in the presence of RNaseOUT RNase inhibitor (40 units/μl; Invitrogen). The reaction was inactivated by heating at 70 °C for 15 min. A 450-bp region of NHA2 was amplified to detect expression and GAPDH (250 bp) was used as loading control.

Li^+ Sensitivity Assays

A) The effect of LiCl on the growth of MDCK cell line was evaluated by MTS cell proliferation assay. Equal numbers of control and NHA2-GFP cells were plated in a 96-well plate in MEM medium, supplemented with 10% FBS and 5% antibiotic-antimycotic solution (referred to as complete media henceforth). Twenty-four hours after the plating, the growth medium was removed, and cells received freshly prepared complete medium (untreated controls), media containing 40 or 100 mM LiCl with no drug, 200 μM amiloride or 200 μM amiloride and 200 μM phloretin. After 48 h of exposure, growth was monitored using a Celltiter 96 Aqueous One Solution cell proliferation assay kit (Promega, Madison, WI) according to the manufacturer's instructions. B) Control and NHA2-GFP expressing MDCK cells were plated in a 9:1 ratio on a 6-well plate in complete MEM medium. Twenty-four hours after the plating, the growth medium was removed, and cells received freshly prepared complete medium (untreated controls) or media containing 90 mM LiCl for 48 h. The cells were then washed with PBS, trypsinized, resuspended in fresh MEM media and divided into two aliquots. Flow cytometry and Western analysis were used to analyze GFP expression with the aliquots. C) Control MDCK cells were treated with 100 nM aldosterone, 1 μM vasopressin or vehicle control for 4 h after which 90 mM LiCl was added to the culture media. The media was replaced by complete media without the hormones and LiCl after 24 h. The effect of LiCl on the growth of MDCK cell line was evaluated by MTS cell proliferation assay after 48 h.

Intracellular Li^+ Measurement

Control and NHA2-GFP-expressing cells were plated in equal numbers on a 6-well plate. Culture media was replaced with media containing 90 mM LiCl. After 2.5 h, the cells were washed quickly with PBS (twice), lysed in 0.1% Nonidet P-40 lysis buffer (EDTA-free), and sonicated. The lysate was centrifuged at 14,000 rpm for 15 min to remove cell debris. Part of the supernatant was diluted in 35% nitric acid, and the lithium levels were measured by atomic absorption spectroscopy. Remaining lysate was used to measure total cellular protein concentrations (Thermo Scientific Pierce BCA Protein Assay Kit). Intracellular lithium levels were expressed as parts per million per microgram of protein. In a similar experiment, NHA2-GFP-expressing MDCK cells were first pretreated with 200 μM phloretin for 10 min and then exposed to 90 mM LiCl for 2.5 h (with 200 μM phloretin). Intracellular lithium levels were determined as above.

SLC Assay

The method to measure sodium stimulated lithium efflux was based on an adaptation to the technique described by Zerbini *et al.* and Canessa *et al.* in fibroblasts and erythrocytes respectively (13, 14). NHA2-GFP-expressing MDCK cells in a 6-well dish were then loaded with Li^+ by incubation in complete MEM media containing 90 mM LiCl, for 2.5 h. During the last 5 min of incubation, ouabain (100 μM) and bumetanide (100 μM) were added to anticipate the inhibition of the Na^+ pump and of the Na^+-K^+ cotransport, respectively. After washing in cold, choline chloride wash buffer (150 mM choline chloride, 1 mM $MgCl_2$, 10 mM Tris, MOPS, pH 7.4 at 4 °C), cells were incubated in efflux buffer containing 10 mM Tris-MOPS buffer (pH 7.4 at 37"C), 1 mM MgCl, 10 mM glucose, 100 μM ouabain, 100 μM bumetanide, 200 μM DIDS (to block the activity of the anion exchanger), and either 150 mM NaCl or 150 mM choline chloride for 5 or 10 min. Parallel experiments were performed using media with amiloride and/phloretin at final concentrations of 200 μM. To minimize between-assay variability, the number of culture wells was always sufficient to perform the individual comparisons between inhibitors in a single experimental set. After incubation, efflux solutions were removed and transferred to tubes to measure the Li^+ concentration. Li^+ was measured by atomic absorption against Li standards in double distilled water. Cells were washed two times with cold choline chloride wash buffer and lysed using 0.1% Nonidet P-40 lysis buffer to measure total cellular protein. Lithium efflux was finally expressed in parts per million per milligram of protein.

Measurement of $Na^+(Li^+)/H^+$ Exchange Activity

A. Na^+-dependent H^+ Efflux—The rate of Na^+-dependent recovery of pHi from an acid load, equivalent to the rate of Na^+/H^+ exchange, was determined at the cellular level by measuring the fluorescence emission of BCECF (a pH-sensitive dye) using dual-wavelength excitation as described previously (15, 16). Briefly, MDCK cells (control and NHA2-GFP cells) were grown to a confluence of ~80% on glass coverslips. The cells were loaded with 4.2 mM BCECF acetoxymethyl ester (BCECF/AM) for 20 min at 37 °C and mounted in a specially designed perfusion chamber. The chamber was placed on the stage of fluorescence spectrophotometer (Photon Technology Quantamaster). Cells were constantly perfused using a gravity-driven system. BCECF fluorescence emission (collected at 530 nm) was measured in response to sequential excitation at two excitation wavelengths, 440 nm and 490 nm. Fluorescence data were recorded every 3.4 s by irradiating the cells for 7 ms at each of the excitation wavelengths. Data were processed and corrected for autofluorescence (measured from cells not loaded with BCECF). Calibration of the BCECF fluorescence ratio *versus* pH_i was performed in the presence of 0.5 mM of the K^+/H^+ ionophore nigericin (in "K-clamp media" of varying pH values, see below) according to a protocol described previously (15–17). For study of Na^+/H^+ exchange activity cells were pulsed with NH_4Cl (40 mM NH_4Cl in TMA-medium, for 20 min). Removal of NH_4Cl and perfusion with "TMA-medium" resulted in acidification of the cells. Acid-loaded cells were then exposed to Na^+ ("Na medium" see later) and the initial rate of pHi recovery was used for quantification of Na^+/H^+ exchange activity. NHE agonist, HOE 694, was introduced during perfusion with Na-medium and the initial rate of pH_i recovery was compared with control experiments without the agonist. Concentration of agonist (50 mM) was chosen to be the same, as determined previously to elicit maximal or near-maximal responses. It has been previously established that MDCK cells tolerated at least three consecutive NH_4Cl pulses without a major fatigue effect on plasma membrane Na^+/H^+ exchange activity (16).

Solutions included: Na-medium: 130 mM NaCl, 1 mM $CaCl_2$, 1 mM $MgSO_4$, 4 mM KCl, 1 mM NaH_2PO_4, 18 mM D-glucose, 20 mM HEPES buffered to pH 7.4 with NaOH; TMA-medium: 130 mM tetramethylammonium-Cl, 1 mM $CaCl_2$, 1 mM $MgSO_4$, 4 mM KCl, 1 mM TMA-PO4, 18 mM D-glucose, 20 mM HEPES buffered to pH 7.4 with TMA-OH; K-clamp-medium: 20 mM NaCl, 110 mM KCl, 1 mM $CaCl_2$, 1 mM $MgSO_4$, 4 mM KCl, 1 mM TMA-PO_4, 18 mM D-glucose, 20 mM HEPES buffered to pH 7.4 with NaOH.

B. H^+-dependent Li^+ Influx—Control and NHA2-GFP cells were incubated in complete MEM medium with 138 mM NH_4Cl for 30 min. During the last 10 min of incubation, ouabain (100 μM) and bumetanide (100 μM) were added. The cells were then washed in cold choline chloride wash buffer (150 mM choline chloride, 1 mM $MgCl_2$, 10 mM Tris, MOPS, pH 7.4 at 4 °C), and incubated in lithium influx buffer containing 10 mM Tris-MOPS buffer (pH 7.4 at 37"C), 1 mM MgCl, 10 mM glucose, 100 μM ouabain, 100 μM bumetanide, 200 μM DIDS, and 90 mM LiCl for 10 min. The cells were then washed twice with cold choline chloride wash buffer and lysed in EDTA-free, 0.1% Nonidet P-40 lysis buffer. Cell debris was removed by centrifuging the lysate for 15 min at 14,000 rpm, and the supernatant was divided into two aliquots. One aliquot was used to measure the Li^+ concentration by atomic absorption spectroscopy and the second aliquot was used to measure protein concentration. Lithium influx was finally expressed in parts per million per milligram of protein.

C. H^+-dependent Li^+ Efflux—NHA2-GFP-expressing MDCK cells in a 6-well plate were loaded with 90 mM Li^+ complete MEM media for 2.5 h. During the last 10 min of incubation, ouabain (100 μM), bumetanide (100 μM), and 200 μM amiloride

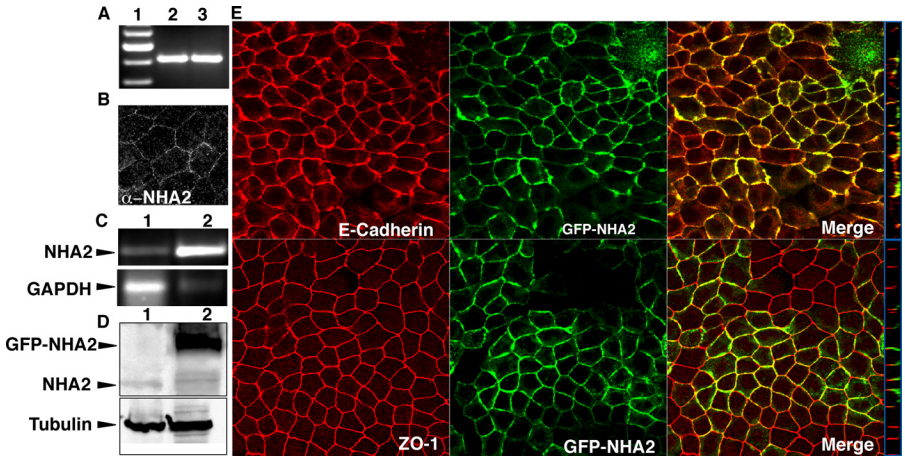

FIGURE 1. **NHA2 expression and localization in MDCK cells.** *A*, reverse transcription-PCR of NHA2 in MDCK cells (*lane 1*), control plasmid (*lane 2*). *B*, immunostaining of endogenous NHA2 using anti-NHA2 antibody. *C*, reverse transcription-PCR comparing NHA2 expression from control cells (*top panel*, *lane 1*) with stably transfected cells overexpressing NHA2-GFP (*top panel*, *lane 2*); *bottom panel*: GAPDH controls. *D*, Western blot of total protein from control cells (*top panel*, *lane 1*) and stably transfected clone overexpressing NHA2-GFP (*top panel*, *lane 2*) using anti-NHA2 and anti-GFP antibodies; *bottom panel*: tubulin controls. *E*, confocal microscopic images; *top panel*: NHA2-GFP (*green*) colocalizes with basolateral marker E-Cadherin (*red*); *bottom panel*: NHA2-GFP (*green*) is found basolateral to the tight junction marker ZO-1 (*red*). *Blue boxes* on the *right* show an orthogonal view of a slice from the confocal image.

were added. The cells were then washed in cold choline chloride wash buffer (150 mM choline chloride, 1 mM $MgCl_2$, 10 mM Tris, MOPS, pH 7.4 at 4 °C), and incubated in lithium efflux buffer at pH 5.5 or 7.4, containing 10 mM Tris-MOPS buffer, 1 mM MgCl, 10 mM glucose, 100 μM ouabain, 100 μM bumetanide, 200 μM DIDS, and 200 μM amiloride for 10 min. The lithium concentrations in the efflux buffers were determined by atomic absorption spectroscopy and normalized to total cellular protein levels as described above.

D. Li^+-dependent H^+ Influx—MDCK cells were grown to a confluence of ~80% on glass coverslips and loaded with 90 mM Li^+ in complete MEM media for 2.5 h. In the last 20 min, 4.2 mM BCECF acetoxymethyl ester (BCECF/AM) was added. Inhibitors, ouabain (100 μM), bumetanide (100 μM), amiloride (200 μM), and bafilomycin (5 nM) with or without phloretin (200 μM) were added during the last 10 min of lithium loading. The coverslips were then mounted in a specially designed perfusion chamber as described above. The cells were then perfused with choline chloride wash buffer (150 mM choline chloride, 1 mM $MgCl_2$, 10 mM Tris, MOPS, pH 7.4 at 4 °C) for ~200 s following which the buffer was switched to an acidic efflux buffer (pH 6.35) containing 10 mM Tris-MOPS buffer, 1 mM MgCl, 10 mM glucose, 100 μM ouabain, 100 μM bumetanide, 200 μM DIDS, 200 μM amiloride, and 5 nM bafilomycin with or without phloretin (200 μM). Calibration of the BCECF fluorescence ratio *versus* pH_i was performed and the rate of pH_i recovery were calculated as described above in (A).

Acid Suicide

The method to measure lithium-stimulated proton influx was based on an adaptation to the technique described by Pouyssegur *et al.* (18). MDCK cells were first incubated for 2 h in 90 mM LiCI buffer (pH 7.4) at 37 °C in the absence of CO_2 (18). These Li^+-loaded cells were then washed twice with 90 mM choline chloride (pH 7.4), and transferred at 37 °C to 90 mM choline chloride acid solution (pH 5.5) for 1 h. For acid suicide study in the presence of NHE and NHA2 agonists, a similar protocol was adopted, but the cells were pretreated with 200 μM amiloride or phloretin treated for 10 min. The cells were then loaded with 90 mM Li and moved choline chloride solution as before. Amiloride or phloretin were also present during the lithium loading and in the choline chloride solution. Cells surviving acid suicide were then incubated in complete MEM media overnight at 37 °C (with 5% CO_2), and cell survival was measured by MTS assay.

Bafilomycin Sensitivity

Equal numbers of control and NHA2-GFP cells were plated in a 96-well plate in complete MEM media. Twenty-four hours after the plating, the growth medium was removed, and cells received freshly prepared complete medium (untreated controls) or media containing 100 mM LiCl with no drug or 5 nM bafilomycin. After 48 h of exposure, growth was monitored using MTS assay.

Coimmunoprecipitation

Coimmunoprecipitation in stable MDCK cells was performed 72 h after seeding cells. Cells were lysed in Nonidet P-40 lysis buffer. Cell lysate was incubated 4 h with GammaBind Plus Sepharose (GE Healthcare, Waukesha, WI) for preclearance and 3 h with anti-NHA2 and anti-VATPase a1 antibodies (2 μg/0.5 ml lysate) at 4 °C. IgG, nonspecific antibody was added to the negative control samples. Beads were washed using lysis buffer containing 1% Nonidet P-40 before SDS-PAGE and immunoblotting. The blots were probed with anti-NHA2, anti-VATPase a1, or anti-VATPase B1/B2 antibodies used at 1:100 dilution. Clean-blot IP detection reagent (Thermoscientific) was used to detect the primary antibodies on the Western blots without interference from denatured IgG.

Statistical Analysis

All plotted data were replicated at least three times independently and the mean ± S.D. is shown. Statistical significance was assessed using the Student's *t* test, and $p < 0.05$ considered significant.

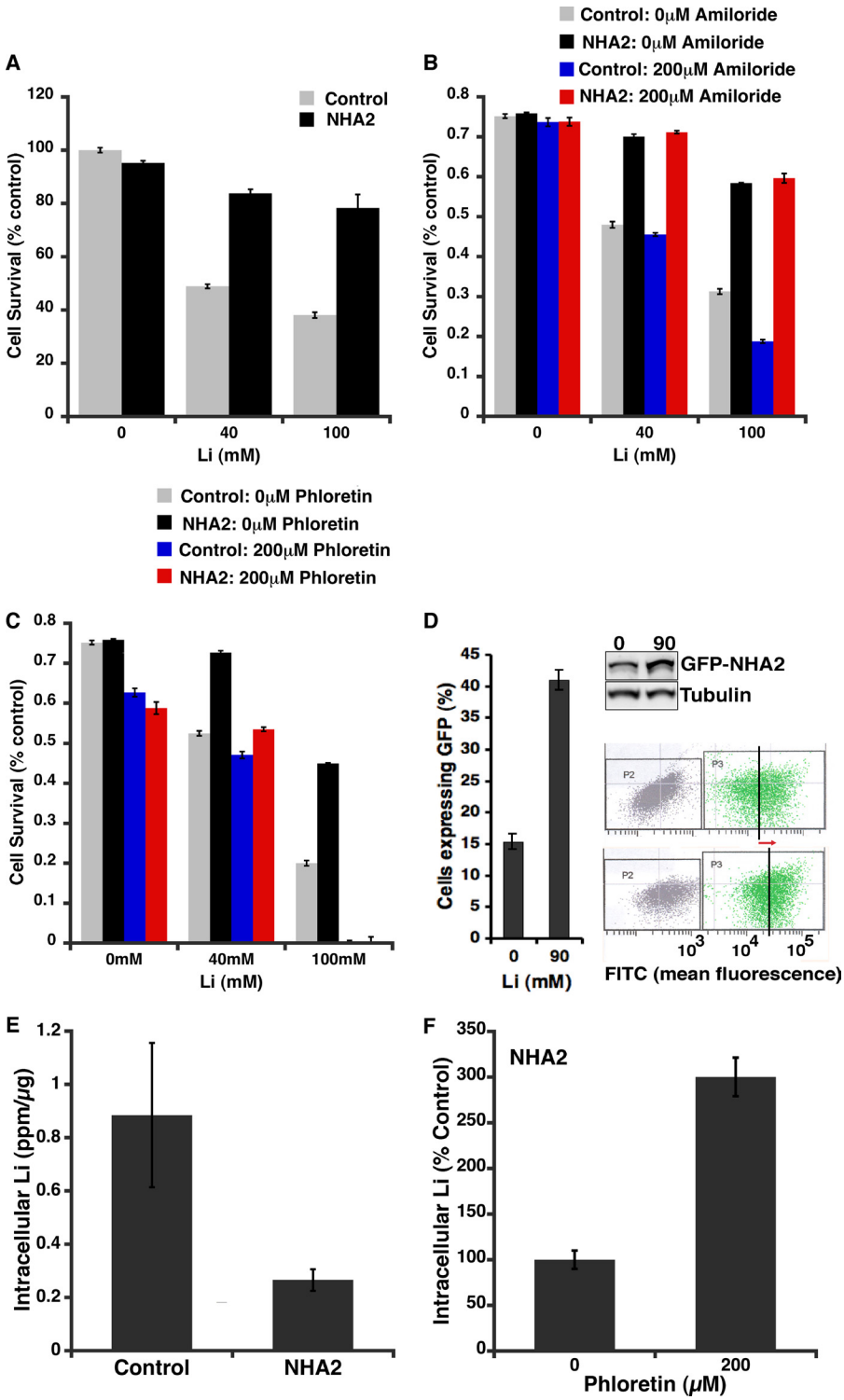

FIGURE 2. **NHA2 confers phloretin-sensitive Li^+ tolerance.** *A*, cell survival was monitored by MTT assay on MDCK cells grown in various Li^+ concentrations. *B*, Li^+ tolerant growth was measured by MTT assay, on control (*gray* and *black*) and MDCK cells overexpressing NHA2 (*maroon* and *red*) in 0 μM (*gray* and *maroon*) and 200 μM (*black* and *red*) amiloride. *C*, Li^+ tolerant growth was measured by MTT assay same as in *B*, but in 0 μM (*gray* and *maroon*) and 200 μM (*black* and *red*) phloretin. *D*, control and NHA2-GFP-overexpressing cells were seeded in a 9:1 ratio, respectively and grown for 48 h in medium supplemented with 0 or 90 mM LiCl. Cells expressing GFP were analyzed by flow cytometry (*left panel*) and Western blot (*inset*). GFP fluorescence as observed by flow cytometry is plotted on a log-axis (*right panel*), and the mean intensity is indicated (*black line*). *Red arrow* indicates a shift in the mean fluorescence intensity. *E*, control and MDCK cells overexpressing NHA2 were loaded with 90 mM Li^+ for 2.5 h. Intracellular Li^+ concentrations measured by atomic absorption spectroscopy (*AAS*) and normalized to total cellular protein. *F*, NHA2-overexpressing MDCK cells were pretreated with 0 or 200 μM phloretin before loading the cells with Li^+ for 2.5 h. Intracellular Li^+ concentrations were measured by AAS and normalized to total cellular protein. Phloretin was also present during Li^+ loading. Mean ± S.D. is shown for all data.

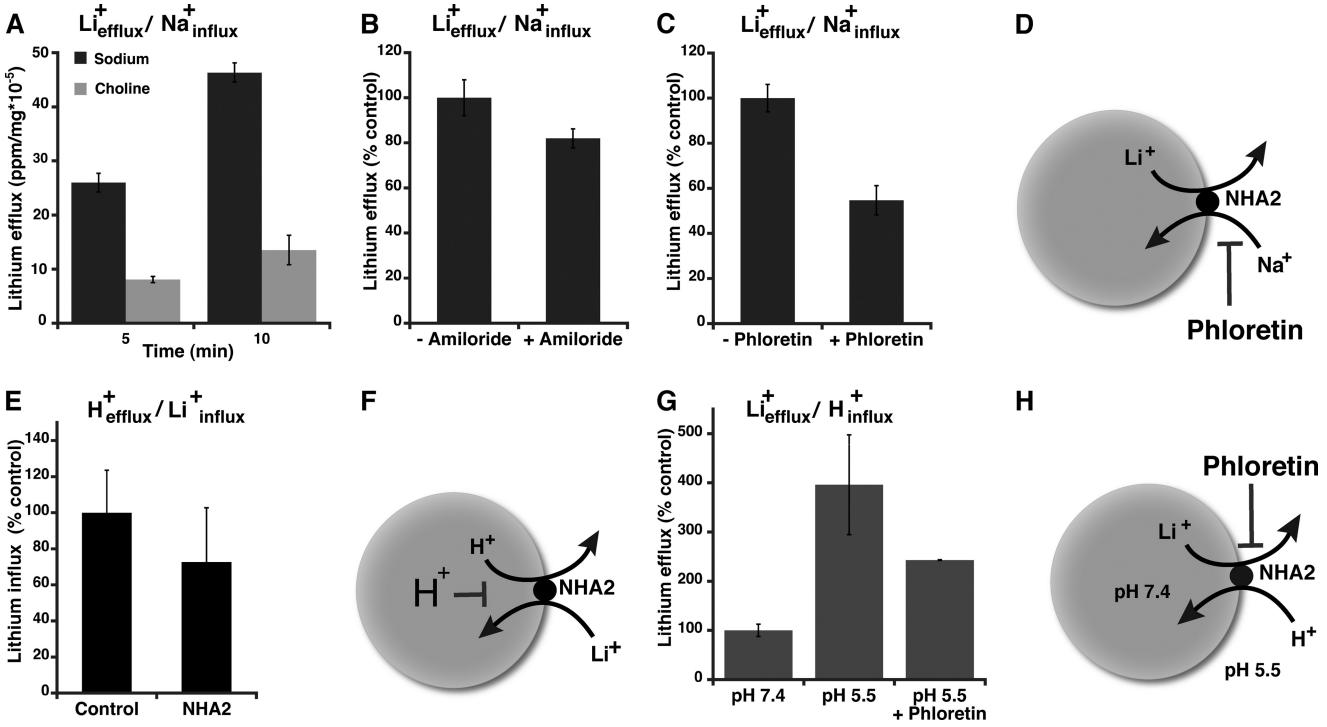

FIGURE 3. **Cation exchange and asymmetric transport modes of NHA2.** *A*, sodium lithium countertransport (*SLC*). MDCK cells overexpressing NHA2 were loaded with Li^+ as described under "Experimental Procedures" and incubated in efflux buffer containing either 150 mM NaCl (*black*) or choline chloride (*gray*) for 5 and 10 min. Li^+ efflux was measured by AAS and normalized to total cellular protein. *B*, SLC activity was measured as described in *A*, in the presence or absence of 200 μM amiloride. *C*, SLC activity was measured as in *A*, in the presence of 200 μM amiloride and 0 or 200 μM phloretin. *D*, model of SLC activity. *E*, cells were acidified by incubation in NH_4Cl followed by incubation in Li^+-supplemented buffer for 10 min, as described under "Experimental Procedures." There was no significant difference in cellular Li^+ in control or NHA2-overexpressing cells. *F*, model of acid inactivation of NHA2. *G*, NHA2-overexpressing cells were loaded with 90 mM Li^+ in the presence of inhibitors including 200 μM amiloride followed by incubation in buffer at pH 7.4 or pH 5.5 (± phloretin) for 10 min. *H*, model of $Na^+(Li^+)_{in}/H^+_{out}$ exchange by NHA2. Mean ± S.D. is shown for all data.

RESULTS

NHA2 Confers Selective Growth Advantage in High Li^+—Madin-Darby canine kidney (MDCK) cells are widely used to investigate renal physiology (19). Confluent monolayers of MDCK cells have Na^+ transport properties similar to mammalian distal nephron (19, 20). We show endogenous expression of NHA2 in MDCK cells by RT-PCR (Fig. 1*A*), immunofluorescence (Fig. 1*B*) and Western blotting (Fig. 1*D*). Next, we established a stable MDCK cell line expressing GFP-tagged NHA2 (Fig. 1, *C* and *D*). We observed colocalization of NHA2-GFP with the basolateral membrane marker E-cadherin (Fig. 1*E*, *top*). Distribution of NHA2-GFP was restricted to the basolateral side of the tight junction marker ZO-1 (Fig. 1*E*, *bottom*).

Using heterologous expression in yeast, we had previously shown that NHA2 conferred robust growth resistance to Li^+ (and Na^+) toxicity (1). Here, we asked whether NHA2 conferred salt tolerance in mammalian cells as well. We used Li^+ as a surrogate for Na^+ ions because it is toxic at lower concentrations, thus avoiding secondary osmotic effects of high salt. We showed that NHA2-GFP increased cell survival in media supplemented with 40 or 100 mM LiCl, relative to control MDCK cells (Fig. 2*A*). Growth was insensitive to amiloride (Fig. 2*B*), a well-known inhibitor of the NHE family. Previously, we had shown that salt tolerance conferred by NHA2 in yeast was sensitive to phloretin, an inhibitor of sodium lithium countertransport. Similarly, phloretin reversed the growth advantage conferred by NHA2 in 40 mM LiCl (Fig. 2*C*). Although phloretin was only mildly toxic to cells in medium lacking LiCl, it was lethal in the presence of 100 mM LiCl, suggesting a requirement for NHA2 function under these conditions (Fig. 2*C*).

These results were surprising because conventional NHE-like cation/H^+ exchange activity was expected to equilibrate Li^+ across the membrane, whereas growth advantage is indicative of active cation efflux. To confirm these findings, we followed the growth of mixed cultures of NHA2-GFP-expressing cells and control cells seeded in a 1:9 ratio. After 48 h, these ratios remained relatively similar in standard medium, but in the presence of 90 mM LiCl, NHA2-GFP cells were enriched by nearly 3-fold at the expense of control cells, as determined by flow cytometry (Fig. 2*D*) and Western analysis (inset). Furthermore, mean fluorescence intensity of GFP-positive cells increased (from 22,613 ± 1,205 to 31,955 ± 781 a.u.) upon LiCl treatment (Fig. 2*D*). Consistent with these findings, NHA2-GFP cells were found to retain correspondingly less (~3.3-fold) intracellular Li^+ relative to control cells following 2 h exposure to LiCl (Fig. 2*E*). Again, treatment with phloretin reversed this difference (Fig. 2*F*), as expected for NHA2 inhibition. Taken together, these results show that NHA2 functions in effect as a phloretin-sensitive Li^+ efflux pump.

NHA2 Has SLC Activity—Elevated SLC activity is a secondary metabolic indication of an underlying cell membrane abnormality associated with essential hypertension (21). The exchange of intracellular Li^+ for Na^+ has been extensively documented in erythrocytes and fibroblasts (13, 14). We moni-

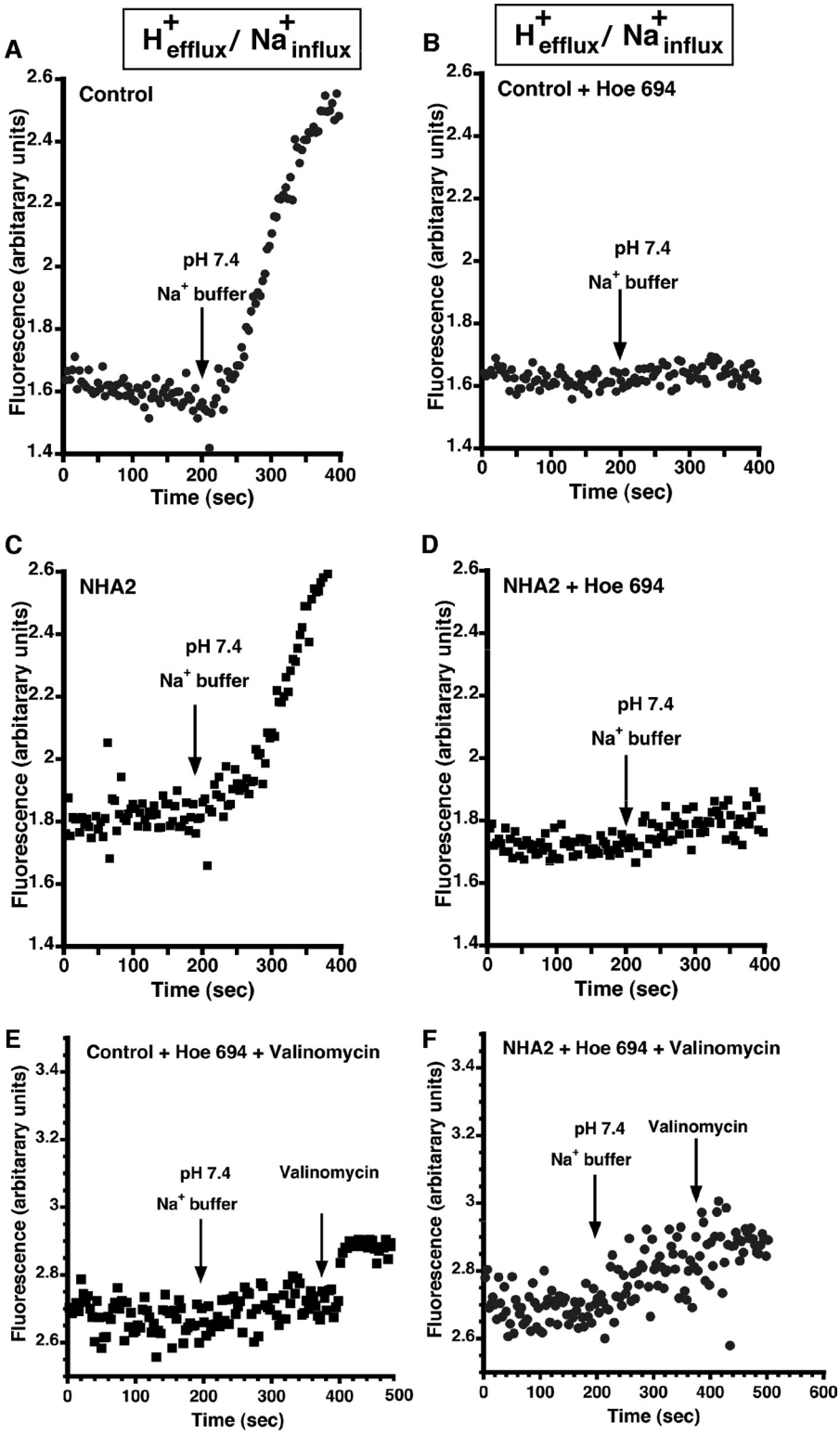

FIGURE 4. **Na^+-dependent H^+ efflux.** *A*, MDCK cells were incubated in NH_4Cl for 30 min as described under "Experimental Procedures." BCECF (4.2 mM) was added in the last 20 min of the loading. The cells were then perfused with "TMA-medium" for 200 s resulting in acidification of the cells following which the buffer was switched to a Na^+ efflux buffer (pH 7.4) *B*, same as *A* except that NHE agonist, HOE 694, was introduced during perfusion with Na-medium. *C*, same as *A* with NHA2-overexpressing MDCK cells. *D*, same as *B* with NHA2-overexpressing MDCK cells. *E*, same as *B*, except 200 s after addition of HOE 694, valinomycin was added to relieve membrane potential differences in HOE694-treated cells. *F*, same as *E* with NHA2-overexpressing MDCK cells.

tored Li^+ efflux in cells stably transfected with NHA2-GFP and preloaded with Li^+ for 2.5h, as described earlier (14). We show that time-dependent Li^+ efflux is 3 times higher in the presence of external Na^+, compared with equivalent concentrations of choline chloride (Fig. 3*A*). Thus, NHA2 mediates $Li_{efflux}{}^+$/ $Na_{influx}{}^+$ exchange as illustrated in Fig. 3*D*. Li^+ efflux in Na^+

containing medium was not significantly affected by the addition of amiloride but was inhibited by phloretin (Fig. 3, *B–D*). Thus, NHA2 mediates SLC activity (Fig. 3*D*) with inhibitor characteristics previously reported in red blood cells, as a marker of hypertension.

NHA2 Is Inactivated by Intracellular Acidification and Does Not Mediate Cation-driven H^+ Efflux—Plasma membrane NHE1 transports H^+ out of the cell, in exchange for Na^+ influx (9, 22). Indeed, this is the conventional direction for active secondary transport in all metazoan cells, powered by an inwardly directed Na^+ gradient. We attempted to measure similar transport by NHA2-GFP in MDCK cells loaded with H^+ and in the presence of external Na^+. Following acute acid load using NH_4Cl prepulse, Na^+-dependent intracellular pH (pH_i) recovery was monitored fluorometrically using the pH-sensitive dye BCECF. Despite the favorable ion gradients in both directions ($H_{efflux}^+/Na_{influx}^+$), there was no significant difference in rates of pH_i recovery (*i.e.* H^+ efflux) between control and NHA2-GFP-overexpressing cells (Fig. 4, *A* and *C*; 0.14 ± 0.0312 and 0.16 ± 0.0282 ΔpH units/minute, respectively). HOE694, a known inhibitor of NHE1, inhibited pH_i recovery completely in both control and NHA2-GFP-overexpressing cells, indicating that pH_i recovery was solely due to NHE activity (Fig. 4, *B* and *D*). We considered the possibility that NHA2 was electrogenic, exchanging $2H^+/Na^+$ like *E. coli* NhaA (11). However, there was no significant pH_i recovery upon addition of K^+/valinomycin to relieve membrane potential differences in HOE694-treated cells (Fig. 4, *E* and *F*). In parallel experiments, we monitored Li^+ influx under similar acid-loaded conditions ($H^+_{efflux}/Li^+_{influx}$) and failed to see a significant increase in Li^+ entry in NHA2-GFP cells, relative to control (Fig. 3*E*). Thus, NHA2 does not show NHE1-like transport activity. Furthermore, these results suggest a model in which NHA2 is inhibited by cytoplasmic acidification and operates at a pH range distinct from NHE (Fig. 3*F*).

NHA2 Mediates Cation Efflux with an Inwardly Directed pH Gradient—Next, we investigated H^+-dependent cation efflux, which is the physiologically reverse mode of plasma membrane NHE. Following preloading with Li^+ at pH 7.4, NHA2-GFP-expressing cells were placed in Na^+-free buffer at pH 7.4 or pH 5.5. We show that Li^+ efflux within the first 10 min was ~4-fold higher with an inwardly directed H^+ gradient, and was sensitive to phloretin (Fig. 3*G*). It is worth noting that this mode of antiport ($Li_{efflux}^+/H_{influx}^+$; Fig. 3*H*) is similar to the physiological mode of bacterial NhaA orthologs and recapitulates our previous results from heterologous expression of NHA2 in yeast (1). In addition, H^+-driven Li^+ efflux could potentially explain the gain in Li^+ tolerant growth conferred by NHA2-GFP demonstrated in Fig. 2, *A* and *D*.

NHA2 Confers Tolerance to Acid Suicide—To investigate the difference between NHA2 and NHE further we subjected control and NHA2-GFP cells to an acid suicide protocol, originally described by Pouyssegur *et al.* to isolate cells lacking plasma membrane NHE function (18). In this scenario, cells are loaded with Li^+ and placed in a low pH environment (Fig. 5*A*). Cell death would be consistent with $Li_{efflux}^+/H_{influx}^+$ exchange activity. Surprisingly, NHA2 conferred tolerance to acid suicide. When Li^+-loaded cells were placed in pH 5.5 buffer followed by outgrowth in normal medium, cell survival was 2-fold greater in the stable line expressing NHA2-GFP, relative to control MDCK cells (Fig. 5*B*). Given the results from Fig. 2*E*, we concluded that reduced accumulation of Li^+ in NHA2-GFP cells conferred protection against acid suicide. Addition of amiloride prior to external acidification also protected both cell lines, consistent with a role for NHE1 in mediating acid suicide as described by Pouyssegur *et al.* (Fig. 5*C*). In contrast, phloretin was lethal to both cell lines under these conditions (Fig. 5*C*). These experiments suggest that NHA2 protects against cytosolic acidification whereas NHE1 promotes it. Thus two subtypes of cation/proton antiporter within the same superfamily exhibit strikingly opposite behavior.

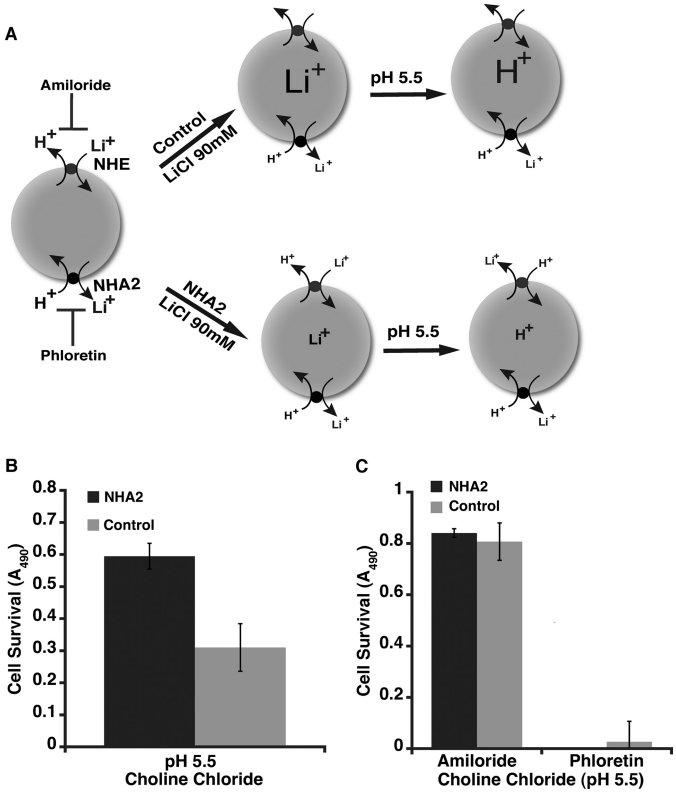

FIGURE 5. **NHA2 protects against acid suicide.** *A*, model depicting the acid suicide experiment. *B*, control and NHA2-overexpressing MDCK cells were loaded with 90 mM Li^+ as described under "Experimental Procedures," then washed with choline chloride (pH 7.4) buffer and transferred to 90 mM choline chloride acid solution (pH 5.5) for 1 h. Cell survival was measured by MTS assay. *C*, acid suicide study in the presence of NHE and NHA2 agonists, a similar protocol as in *B* was adopted but the cells were pretreated with 200 μM amiloride or phloretin for 1 h prior to Li^+ loading. Amiloride or phloretin were also present during the lithium loading and in the choline chloride solution. Cell survival was measured by MTS assay. Mean ± S.D. is shown for all data.

NHA2 Is Coupled with the V-ATPase to Function as a Virtual Cation Efflux Pump—Our findings can be explained by a model in which active cation efflux by NHA2 is coupled to a primary H^+ gradient at the plasma membrane. A candidate H^+ pump in mammalian cells is the lyso/endosomal V-type H^+-ATPase that has been observed on the plasma membrane in cells specialized to secrete protons, including osteoclasts and the intercalated cells of the kidney collecting duct (23, 24). To test this hypothesis, we investigated the effect of bafilomycin, a specific V-ATPase inhibitor, on the Li^+ tolerant phenotype conferred

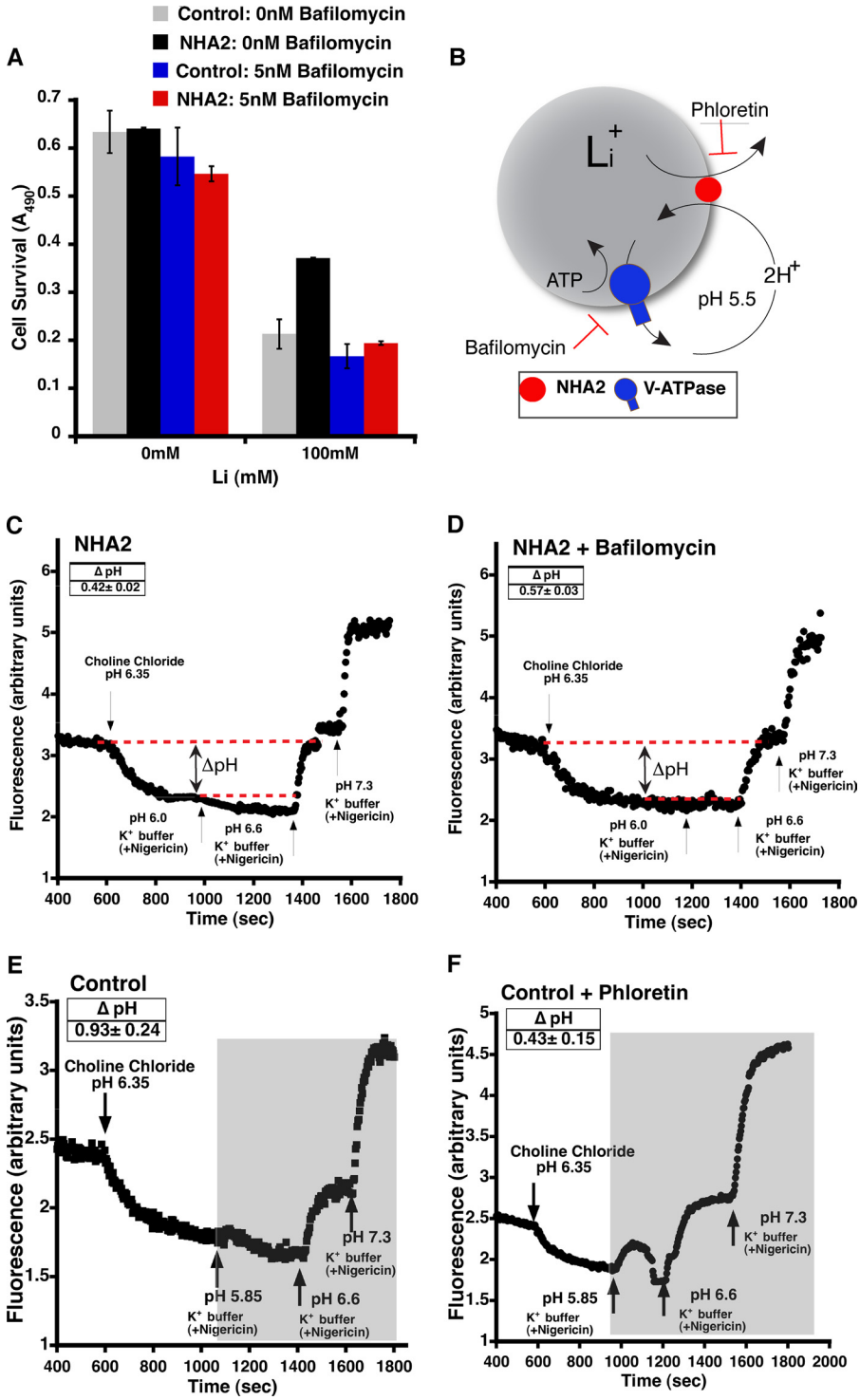

FIGURE 6. **Functional coupling of NHA2 with V-ATPase.** *A*, inhibition of V-ATPase abolished NHA2-mediated Li^+ tolerant growth. Growth, measured by MTT assay, on control (*gray* and *black*) and MDCK cells overexpressing NHA2 (*maroon* and *red*) in 0 nM (*gray* and *maroon*) and 5 nM (*black* and *red*) bafilomycin. *B*, model for V-ATPase driven cation efflux by NHA2. Cation stoichiometry is based on *E. coli* NhaA. *C*, MDCK cells overexpressing NHA2 were loaded with 90 mM Li^+ for 2.5 h. BCECF (4.2 mM) was added in the last 20 min of the loading. Ouabain, bumetanide, DIDS, and amiloride were also added as described under "Experimental Procedures" during the last 10 min of lithium loading. The cells were then perfused with choline chloride wash buffer for 200 s following which the buffer was switched to an acidic efflux buffer (pH 5.5). Calibration of the BCECF fluorescence ratio *versus* pH_i was performed, and ΔpH (*red dotted line*) was calculated as described under "Experimental Procedures." *D*, same as *A* except that Bafilomycin was added along with ouabain, bumetanide, DIDS, and amiloride. *E*, MDCK cells were loaded with 90 mM Li^+ for 2.5 h. BCECF (4.2 mM) was added in the last 20 min of the loading. Bafilomycin, ouabain, bumetanide, DIDS, and amiloride were also added as described under "Experimental Procedures" during the last 10 min of lithium loading. The cells were then perfused with choline chloride wash buffer for 200 s following which the buffer was switched to an acidic efflux buffer (pH 5.5). Calibration of the BCECF fluorescence ratio *versus* pH_i was performed, and ΔpH was calculated as described under "Experimental Procedures." *F*, same as *E* except that the cells were also treated with 200 μM phloretin, beginning during the last 10 min of Li^+ loading. Mean ± S.D. is shown for all data.

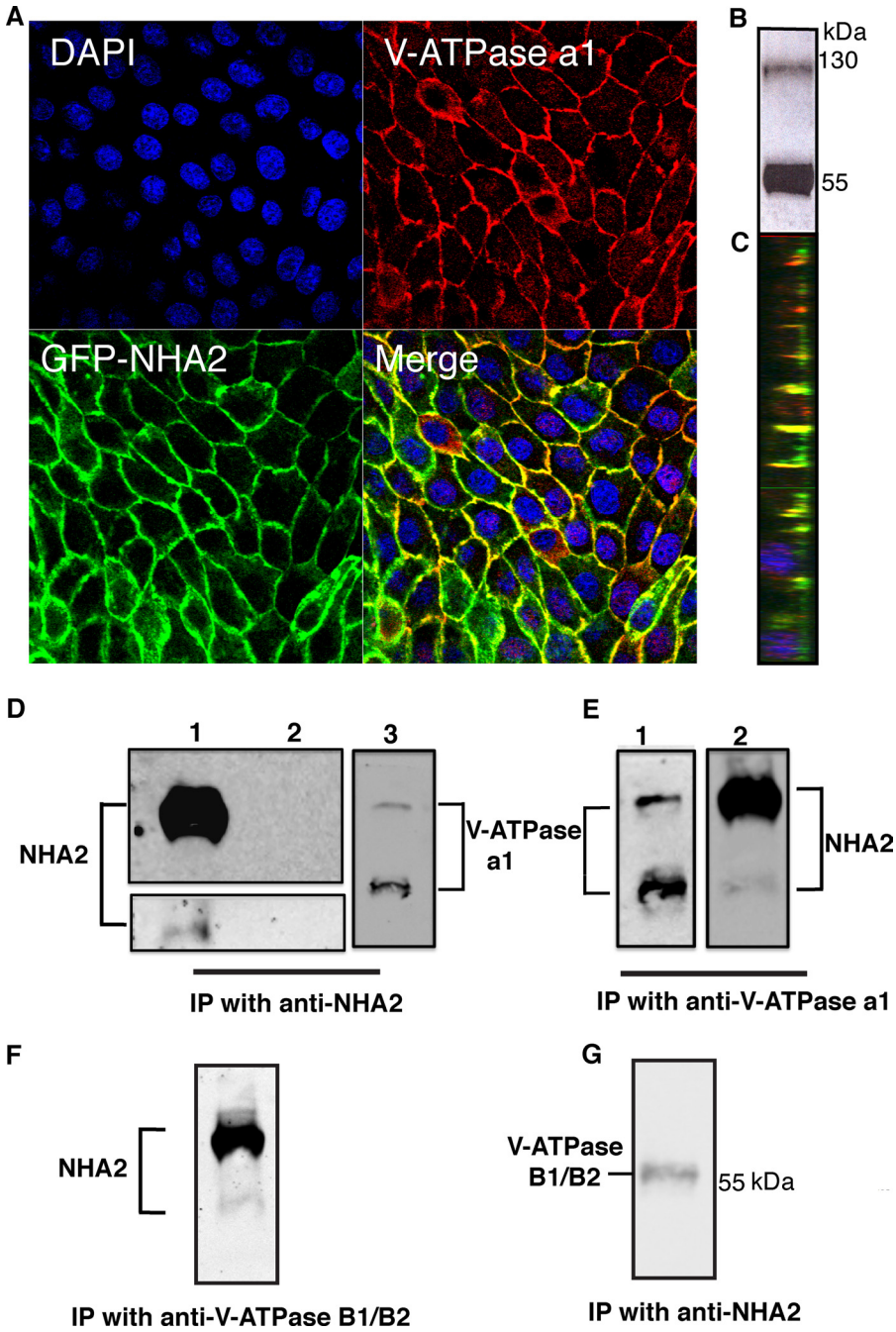

FIGURE 7. **Physical coupling of NHA2 with V-ATPase.** *A*, confocal microscopic images showing colocalization of NHA2-GFP with V-ATPase. Nuclei stained by DAPI (*blue*), indirect immunofluorescence of V-ATPase a1 (*red*), and NHA2-GFP (*green*). *B*, Western blot of MDCK cells using anti V-ATPase a1 antibody, showing expression of V-ATPase in MDCK cells. *C*, orthogonal view of a slice from the merged confocal image (from *A*) showing basolateral colocalization of V-ATPase and NHA2-GFP in MDCK cells. *D*, coimmunoprecipitation (*Co-IP*) using anti-NHA2. Western blot of Co-IP probed with: 1) Anti-NHA2 antibody showing NHA2-GFP (*lane 1*, *top panel*), endogenous NHA2 (*lane 1*, *bottom panel*) and IgG control (*lane 2*). 2) Anti-V-ATPase a1 antibody showing the ~116 kDa V-ATPase a1 band (*lane 3*). *E*, co-IP using anti-V-ATPase a1 antibody: Western blot of Co-IP probed with 1) Anti-V-ATPase a1 antibody (*lane 1*). 2) Anti-NHA2 antibody (*lane 2*). *F*, co-IP using anti-V-ATPase B1/B2 antibody; Western blot of Co-IP probed with anti-NHA2 antibody. *G*, co-IP using anti-NHA2 antibody; Western blot of Co-IP probed with anti-V-ATPase B1/B2 antibody.

by NHA2-GFP overexpression. Bafilomycin, at low concentrations, was not significantly toxic to MDCK cells in the absence of LiCl. However, bafilomycin completely abolished Li^+ tolerance conferred by NHA2-GFP overexpression, suggesting a critical role for the V-ATPase in NHA2 function (Fig. 6*A*). Therefore, we proposed a model in which the proton motive force generated by the V-ATPase drives cation efflux by NHA2 resulting in a combined H^+-cation efflux mechanism (Fig. 6*B*). Consistent with this model, bafilomycin lowered cytoplasmic pH and increased ΔpH (from 0.42 ± 0.02 to 0.57 ± 0.03; Fig. 6, *C* and *D*) in Li^+-loaded NHA2 cells subjected to an inwardly directed H^+ gradient. Also as expected, in MDCK cells that do not overexpress NHA2 and therefore accumulate higher levels of Li^+ upon loading, even larger ΔpH was observed upon extracellular acidification, in the presence of bafilomycin (0.93 ± 0.24). Treatment with phloretin decreased cytoplasmic acidifi-

cation and ΔpH, consistent with inhibition of NHA2-mediated $Li^+_{efflux}/H^+_{influx}$ exchange (Fig. 6, *E* and *F*).

In further support of this model of H^+ driven cation efflux, we show expression and plasma membrane localization of the V-ATPase in MDCK cells (Fig. 7, *A–C*; a1 subunit). Significantly, V-ATPase was found to co-localize with NHA2-GFP on lateral domains of these cells (Fig. 7, *A* and *C*), supporting a functional interaction. Finally, we explored the possibility of association between NHA2 and V-ATPase, at a molecular level. In stably-transfected MDCK cells, V-ATPase robustly coimmunoprecipitated with NHA2 and *vice versa* (Fig. 7, *D* and *E*), consistent with a stable physical interaction between the H^+ pump and NHA2 antiporter.

DISCUSSION

There exists a remarkable multiplicity of genes encoding cation/proton antiporters in mammals. In addition to nine NHE (SLC9A1–9) isoforms belonging to the CPA1 clade, two NHA isoforms (SLC9B1–2) were recently added to the CPA2 clade (25). Of note, all plasma membrane NHE isoforms (NHE1–5) mediate proton efflux powered by an inwardly directed Na^+ gradient established by the ubiquitous Na^+/K^+-ATPase. However, CPA2 family members, represented in metazoan genomes by two genes (NHA1–2), have remained poorly characterized due to lack of functional evidence for transport activity in mammalian cells. Specific efforts by our group and others to uncover Na^+-driven H^+ efflux from acid-loaded cells failed to reveal transport activity of NHA2 (7). These failures can now be explained by our findings showing that, (i) NHA2 is acid-inhibited, in contrast to the NHE antiporters known to be acid-activated, and (ii) NHA2 is chemiosmotically coupled to H^+ rather than Na^+ electrochemical gradients. Thus, NHA2 recapitulates shared phylogenetic origins with distant bacterial NhaA orthologs even in the native mammalian environment. This is consistent with our previous results from mutational analysis in the yeast model, suggesting that common transport and regulation characteristics are preserved within sequence similarities (26).

Our findings are significant and paradigm shifting because it is widely accepted that the vast majority of secondary transport at the plasma membrane of mammalian cells is coupled to the Na^+ electrochemical gradient. This is in contrast to bacteria, fungi, protozoans, and plants, where H^+ gradients drive secondary uptake of solutes and metabolites. H^+ gradients have thus far only been characterized in some specialized cells such as phagocytes, osteoclasts, and kidney-intercalated cells where the V-type H^+-ATPase has been shown to be recruited to the plasma membrane (24). Given the ubiquitous tissue distribution of NHA2, our findings suggest that H^+-coupled transport may be more widespread in the plasma membranes of metazoan cells. The V-ATPase is also a ubiquitously expressed pump, and although best known for lysosomal and endosomal acidification, our results implicate an additional general role in driving secondary transport at the plasma membrane of mammalian cells. In the kidney, under physiological conditions, microdomains of pH gradients may exist near the transporter. For example, acidic microclimate in the small intestine drives the H^+-coupled/pH-dependent transporters like PepT1, PCFT, PAT1, MCT1, and OATP2B1 (27). This is also seen in renal tubules with PepT2 and MATE1 transporters (27). In addition, functional coupling with other transporters is also known to provide pH gradients for H^+-coupled transport both in the small intestine and kidney (27). Diseased conditions such as metabolic or respiratory acidosis may also cause global pH changes that may provide the gradient necessary to drive H^+-coupled transport.

It is noteworthy that in insect epithelia, the electrogenic V-ATPase establishes a membrane potential that drives sensory signaling, fluid secretion, and alkalization (24). In the goblet cell apical membrane of the insect *Manduca sexta*, there is precedence for a hybrid of the V-ATPase and a $K^+/2H^+$ antiporter functioning as a K^+ pump (28). We suggest that functional coupling of NHA2 and V-ATPase establishes a mechanistically novel Na^+ (Li^+) efflux pump in mammalian cells. Cultured MDCK cells retain properties of intercalated cells of the distal nephron (29), where V-ATPase localization is known to alternate between apical and basolateral membranes. It is likely that NHA2 localization is also coupled with that of V-ATPase resulting in a virtual cation-H^+ efflux mechanism to regulate Na^+ homeostasis, volume regulation and consequently, hypertension.

Acknowledgments—We thank Dr. Mark Donowitz and Dr. Varsha Singh for assistance with cytoplasmic pH measurements.

REFERENCES

1. Xiang, M., Feng, M., Muend, S., and Rao, R. (2007) A human Na+/H+ antiporter sharing evolutionary origins with bacterial NhaA may be a candidate gene for essential hypertension. *Proc. Natl. Acad. Sci. U.S.A.* **104,** 18677–18681
2. Carretero, O. A., and Oparil, S. (2000) Essential hypertension. Part I: definition and etiology. *Circulation* **101,** 329–335
3. Weder, A. B. (1986) Red-cell lithium-sodium countertransport and renal lithium clearance in hypertension. *N. Engl. J. Med.* **314,** 198–201
4. Lifton, R. P., Hunt, S. C., Williams, R. R., Pouysségur, J., and Lalouel, J. M. (1991) Exclusion of the Na(+)-H+ antiporter as a candidate gene in human essential hypertension. *Hypertension* **17,** 8–14
5. Canessa, M., Adragna, N., Solomon, H. S., Connolly, T. M., and Tosteson, D. C. (1980) Increased sodium-lithium countertransport in red cells of patients with essential hypertension. *N. Engl. J. Med.* **302,** 772–776
6. Morrison, A. C., Boerwinkle, E., Turner, S. T., and Ferrell, R. E. (2005) Genome-wide linkage study of erythrocyte sodium-lithium countertransport. *Am. J. Hypertens.* **18,** 653–656
7. Fuster, D. G., Zhang, J., Shi, M., Bobulescu, I. A., Andersson, S., and Moe, O. W. (2008) Characterization of the sodium/hydrogen exchanger NHA2. *J. Am. Soc. Nephrol.* **19,** 1547–1556
8. Ecelbarger, C. A., and Tiwari, S. (2006) Sodium transporters in the distal nephron and disease implications. *Curr. Hypertens Rep.* **8,** 158–165
9. Padan, E., Bibi, E., Ito, M., and Krulwich, T. A. (2005) Alkaline pH homeostasis in bacteria: new insights. *Biochim. Biophys. Acta* **1717,** 67–88
10. Padan, E., Kozachkov, L., Herz, K., and Rimon, A. (2009) NhaA crystal structure: functional-structural insights. *J. Exp. Biol.* **212,** 1593–1603
11. Mager, T., Rimon, A., Padan, E., and Fendler, K. (2011) Transport mechanism and pH regulation of the Na+/H+ antiporter NhaA from *Escherichia coli*: an electrophysiological study. *J. Biol. Chem.* **286,** 23570–23581
12. Kallay, L. M., McNickle, A., Brennwald, P. J., Hubbard, A. L., and Braiterman, L. T. (2006) Scribble associates with two polarity proteins, Lgl2 and Vangl2, via distinct molecular domains. *J. Cell. Biochem.* **99,** 647–664
13. Canessa, M. (1995) Red cell sodium-lithium countertransport and cardiovascular risk factors in essential hypertension. *Trends Cardiovasc. Med.* **5,**

102–108
14. Zerbini, G., Mangili, R., Gabellini, D., and Pozza, G. (1997) Modes of operation of an electroneutral Na+/Li+ countertransport in human skin fibroblasts. *Am. J. Physiol.* **272,** C1373–C1379
15. Akhter, S., Cavet, M. E., Tse, C. M., and Donowitz, M. (2000) C-terminal domains of Na(+)/H(+) exchanger isoform 3 are involved in the basal and serum-stimulated membrane trafficking of the exchanger. *Biochemistry* **39,** 1990–2000
16. Helmle-Kolb, C., Di Sole, F., Forgo, J., Hilfiker, H., Tse, C. M., Casavola, V., Donowitz, M., and Murer, H. (1997) Regulation of the transfected Na+/H+-exchanger NHE3 in MDCK cells by vasotocin. *Pflugers Arch.* **434,** 123–131
17. Mohan, S., Tse, C. M., Gabelli, S. B., Sarker, R., Cha, B., Fahie, K., Nadella, M., Zachos, N. C., Tu-Sekine, B., Raben, D., Amzel, L. M., and Donowitz, M. (2010) NHE3 activity is dependent on direct phosphoinositide binding at the N terminus of its intracellular cytosolic region. *J. Biol. Chem.* **285,** 34566–34578
18. Pouysségur, J., Sardet, C., Franchi, A., L'Allemain, G., and Paris, S. (1984) A specific mutation abolishing Na+/H+ antiport activity in hamster fibroblasts precludes growth at neutral and acidic pH. *Proc. Natl. Acad. Sci. U.S.A.* **81,** 4833–4837
19. Wegmann, M., and Nüsing, R. M. (2003) Prostaglandin E2 stimulates sodium reabsorption in MDCK C7 cells, a renal collecting duct principal cell model. *Prostaglandins Leukot Essent Fatty Acids* **69,** 315–322
20. Lahr, T. F., Record, R. D., Hoover, D. K., Hughes, C. L., and Blazer-Yost, B. L. (2000) Characterization of the ion transport responses to ADH in the MDCK-C7 cell line. *Pflugers Arch.* **439,** 610–617
21. Kammerer, C. M., Cox, L. A., Mahaney, M. C., Rogers, J., and Shade, R. E. (2001) Sodium-lithium countertransport activity is linked to chromosome 5 in baboons. *Hypertension* **37,** 398–402
22. Lee, B. L., Sykes, B. D., and Fliegel, L. (2011) Structural analysis of the Na+/H+ exchanger isoform 1 (NHE1) using the divide and conquer approach. *Biochimie Biologie Cellulaire* **89,** 189–199
23. Saroussi, S., and Nelson, N. (2009) Vacuolar H(+)-ATPase-an enzyme for all seasons. *Pflugers Arch.* **457,** 581–587
24. Jefferies, K. C., Cipriano, D. J., and Forgac, M. (2008) Function, structure, and regulation of the vacuolar (H+)-ATPases. *Arch. Biochem. Biophys.* **476,** 33–42
25. Brett, C. L., Donowitz, M., and Rao, R. (2005) Evolutionary origins of eukaryotic sodium/proton exchangers. *Am. J. Physiol. Cell Physiol.* **288,** C223–C239
26. Schushan, M., Xiang, M., Bogomiakov, P., Padan, E., Rao, R., and Ben-Tal, N. (2010) *J. Mol. Biol.* **396,** 1181–1196
27. Anderson, C. M., and Thwaites, D. T. (2010) Hijacking solute carriers for proton-coupled drug transport. *Physiology* **25,** 364–377
28. Harvey, W. R. (2009) Voltage coupling of primary H+ V-ATPases to secondary Na+- or K+-dependent transporters. *J. Exp. Biol.* **212,** 1620–1629
29. Verkoelen, C. F., van der Boom, B. G., Kok, D. J., Houtsmuller, A. B., Visser, P., Schröder, F. H., and Romijn, J. C. (1999) Cell type-specific acquired protection from crystal adherence by renal tubule cells in culture. *Kidney Int.* **55,** 1426–1433